

## REVIEW OF BIO DEGRADABLE PLA IN FUSED DECOMPOSITION 3D MODELING

**Hariom, Phd Scholar**

Department of Mechanical, NIT Patna, Bihar, India.

### *Abstract:*

One of the most common methods of 3D printing—fused deposition modeling (FDM), also known as fused filament fabrication—uses layer-by-layer addition of polymeric materials to form a completed piece. This addition is facilitated by computer-aided design, which instructs the printer where to add polymer. PLA is popular for 3D printing due to its affordability, renewability (e.g., derived from corn or sugar cane), and biocompatibility. Thermal processing conditions also play a key role in sample material properties. For example, samples made with low build platform temperatures have increased mechanical properties, increased interfacial strength, larger crystal size, and lower crystallinity. This review focuses on PLA-based nanocomposites with cellulose, metal-based nanoparticles, continuous fibers, carbon-based nanoparticles, or other additives. These additives impact both the physical properties and printability of the resulting nanocomposites. We also detail the optimal conditions for using these materials in FDM 3D printing. PLA biodegradation depends on pH (degrading faster in highly acidic or basic media), temperature, autocatalytic behavior (catalysis by the lactic acid formed during degradation), and the degree to which water enters the matrix.

**Keywords:** nanocomposites, crystallinity, biocompatibility.

## I. INTRODUCTION

FDM involves drawing a filament through a heated extrusion head, which deposits the molten polymer onto a bed where the 3D-printed part forms [7,8]. The FDM process requires specific parameters for draw ability and process ability that influence not only the filament production but also the layer deposition during printing [9]. For viable printing, the extruded material must have a low melting temperature and fast solidification time [7]. The printability and strength of printed parts also relies on good adhesion between layers and a homogeneous distribution of any additives [10]. Uniform distribution of additives ensures that agglomerates do not clog the printing apparatus or cause weak points in the printed material [11]. Additive manufacturing (3D printing) enables rapid prototyping, convenient customization, and unique capabilities, while democratizing the manufacturing process in ways that are only just beginning to be leveraged on a large scale [1–3]. These burgeoning manufacturing trends, however, also intersect with growing concerns about the ecological impact of the materials used in manufacturing. As pollution from plastic waste grows worldwide, developing materials that are biodegradable and bio-renewable becomes increasingly important [4–6]. Unfortunately, most materials commonly used for 3D printing are

neither. Additionally, PLA is insulating, which precludes its use in conducting parts [19]. To address each of these issues, various additives have been incorporated into PLA to increase its strength and conductivity. In this review we delve into different additives that enhance mechanical, thermal, or electrical properties while maintaining the biodegradability of the resulting PLA/additive nanocomposite.

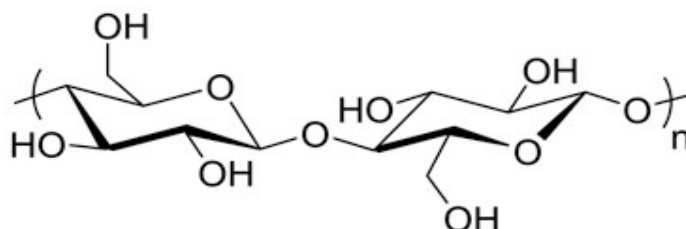


Fig 1: polylactic acid

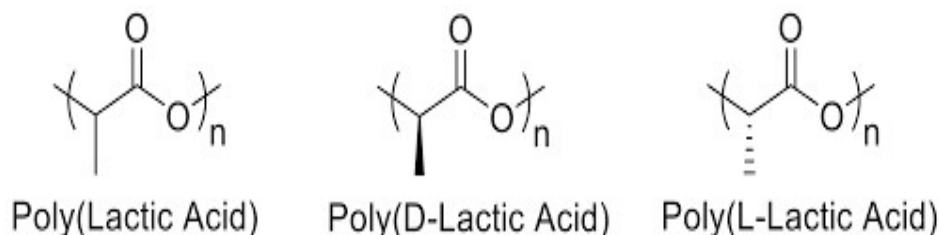


Fig 2: lactic acid

## II. Metal-Based Additives

During processing, the suspended silver nanowires aligned in the direction of shear force homogeneously but broke down. Specifically, the shear force and heat required for 3D printing broke the nanowires into smaller particles but conserved the surface morphology. TGA showed that the nanowires influence the degradation of the PLA matrix: They increased the degradation temperature, increased crystallinity before printing, decreased T<sub>g</sub>, decreased crystallinity after printing, and did not change T<sub>m</sub> [46]. Interestingly, the concentration of nanowires decreased after printing, indicating that some silver nanowires stuck to the inside of the polymer extrusion nozzle. Overall, the addition of silver nanowires added a barrier to degradation of the PLA/Ag nanocomposite while adding an antibacterial property, killing 100% of both *S. aureus* and *E. coli* for all concentrations of silver nanowires studied [46]. Copper fiber/PLA composites contain uneven surface morphologies after FDM 3D printing due to the layer-by-layer addition, which often leaves ridges in the surface of printed materials. To ameliorate the effects of this surface structure, laser polishing is employed to melt the polymer matrix at the surface, producing a smoother surface

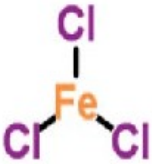

Name	Structure	Molecular formula
FeCl <sub>3</sub>		Cl <sub>3</sub> Fe
Cerium(IV) oxide		CeO <sub>2</sub>

Fig 3: Structure and formula of metal based additives

The surface roughness decreases over 90% after laser treatment to 0.87  $\mu\text{m S}_\alpha$  with a 5 W laser of 200  $\mu\text{m}$  (ideal parameters) as seen in Figure 5. This polishing also significantly improved the glass transition, storage modulus, Young's modulus (34.2%), loss modulus, and tensile strength (52.98%) of Cu/PLA due to strong interfacial adhesion between PLA and Cu fibers after treatment. More recent studies on introducing silver nanoparticles indicate that composites with no significant change in bulk properties can be formed with an addition of 0.01–5 wt % silver nanoparticles. At all loadings of silver nanoparticles studied, these new PLA/Ag nanocomposites showed antimicrobial properties against *E. coli*, *P. aeruginosa*, and *S. aureus* [47]. Many industrial applications cannot use FDM-printed parts because fractures occur between layers due to poor interfacial adhesion and low surface quality. Therefore, modifying FDM PLA nanocomposites to increase this surface quality may increase industrial use of these nanocomposites. Incorporating aluminum into nanocomposites produces air-cooled heat exchangers with high thermal conductivity at a low cost. These PLA/Al composites, when laser polished, show increased surface quality, decreased surface roughness, increased storage modulus, decreased loss tangent, increased tensile strength, and increased Young's modulus.

### III. PLA

PLA biodegradation depends on pH (degrading faster in highly acidic or basic media), temperature, autocatalytic behavior (catalysis by the lactic acid formed during degradation), and the degree to which water enters the matrix [23]. PLA also retains good mechanical strength while remaining process able through melt mixing, solution mixing, injection molding, and 3D printing [21]. However, several drawbacks limit its industrial use such as brittleness, poor thermal stability, low crystallinity, low elongation at break, poor impact strength, low heat-distortion temperature, and limited drawability [9,21,24]. These drawbacks, especially the slow crystallization, deter the replacement of fossil-based thermoplastics with PLA [25]. To increase the functionality of PLA, researchers have introduced additives such as cellulose, metals, carbon, continuous fibers, and others to modulate properties such as thermal conductivity, electrical conductivity, mechanical strength, viscosity, and degradation time [9,26]. s. Chacón et al. investigated the effects of these parameters on the properties of neat

PLA FDM-printed tensile bars as depicted in Figure 2 [27]. Increasing layer thickness increased tensile and flexural strength for upright printed tensile bars. However, on-edge and flat printed tensile bars had only slight differences in the tensile and flexural strength [27,28]. Decreasing feed rate decreased tensile and flexural strength in upright samples but had limited effects on materials produced by on-edge and flat printing orientations. For all samples, the ductility decreased as layer thickness increased.

Overall, on-edge orientation produced the best mechanical performance, ductility, and stiffness. Moreover, if an on-edge orientation is used, high layer thickness and low feed rate maximize ductility [27]. The silylation reaction functionalizes the hydroxyl groups on cellulose, increasing CNW compatibility with PLA. Functionalization also modifies the usable temperatures of the PLA/CNW nanocomposite. The addition of silane A-151 increased the  $T_{max}$  to 304.4 °C [24]. Importantly, the concentration of A-151 must be high enough, at least 8 wt %, to fully coat the CNWs and create an even surface. While silylation increased the compatibility of the PLA and CNWs, the tensile strength and tensile modulus decreased minimally with increasing silane concentration. However, the elongation at break increased significantly (from 12.3% to 213.8%) with increasing silane concentration. The stiffness also increased with silane addition. In general, the tensile strength and tensile modulus increase with silylation of CNWs; however, the thermal properties, including the glass transition temperature, crystallinity, melting temperature, and crystallization temperature, decrease after silylation. Tensile properties increased with infill density regardless of infill pattern. Traditionally, PLA is sold as filaments for FDM with colorants and additives already incorporated. These additives can have profound effects on the properties of the resulting printed material. For example, Cicala et al. observed a marked difference in elasticity among various commercial PLA samples, demonstrating the effect of different additives on mechanical properties [35].

Importantly, Cicala et al. determined that polymers with high viscosity print with increased precision because of their resistance to flow after printing, which allows them to hold their shape and minimize voids between printed layers [35]. Cuiffo et al. investigated commercial PLA samples with calcium carbonate additives and found that the  $CaCO_3$  concentrated in the voids of the 3D-printed materials after FDM printing [36]. Additionally, these PLA samples underwent minor chemical reactions during the FDM process, as shown by changes in the Fourier transform infrared (FTIR) Adding plasticizers such as poly(ethylene glycol) (PEG) into PLA may increase ductility and toughness, but often decreases strength and stiffness [20]. These drawbacks may be mitigated by introducing nucleating agents, such as CNCs or CNFs, which increase the crystallinity of the PLA/PEG matrix and thus increase the strength and stiffness. Adding CNFs and CNCs gives significantly higher crystallinity than neat PLA or commercially available PLA/talc nanocomposites [20]. Solvent effects on CNC dispersion have recently been investigated in both amorphous and semi-crystalline PLA samples. Thermodynamic analysis identified dimethyl sulfoxide/tetrahydrofuran (DMSO/THF) as an

optimal solvent system to incorporate CNCs into PLA because it can both dissolve the PLA and distribute the CNCs [43]. In semi-crystalline PLA nanocomposites, the CNCs distribute effectively but in amorphous nanocomposites the CNCs aggregate [43]. With the addition of CNCs, the storage modulus and complex viscosity increase. Significantly, residual solvent in the nanocomposite matrices caused dramatic decreases in complex viscosity (1 to 2 orders of magnitude) [43].

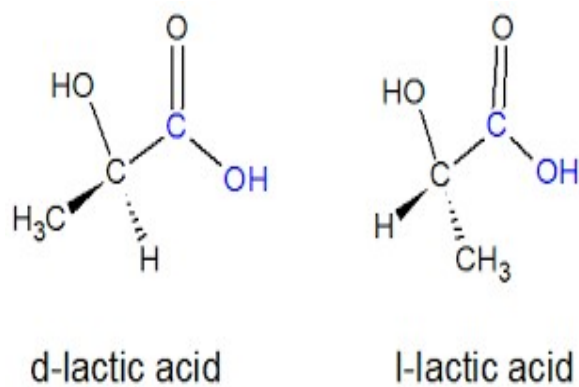


Fig 4: PLA

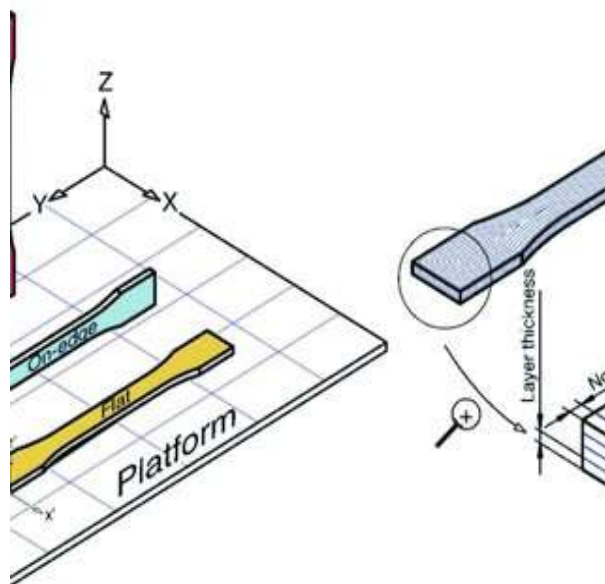


Fig 5: Fused decomposition modeling

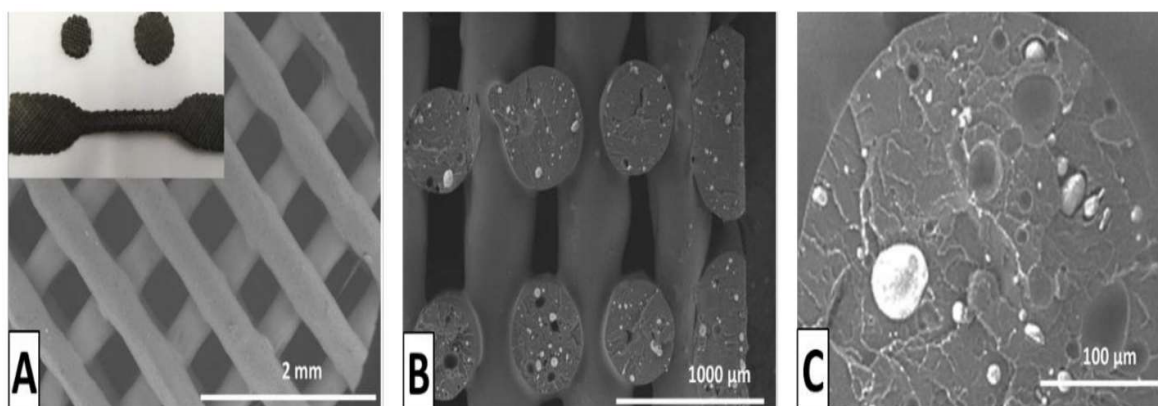


Fig 6: Biodegradable PLA

### III .Cellulose-Based Additives

The silylation reaction functionalizes the hydroxyl groups on cellulose, increasing CNW compatibility with PLA. Functionalization also modifies the usable temperatures of the PLA/CNW nanocomposite. The addition of silane A-151 increased the  $T_{max}$  to 304.4 °C [24]. Importantly, the concentration of A-151 must be high enough, at least 8 wt %, to fully coat the CNWs and create an even surface. While silylation increased the compatibility of the PLA and CNWs, the tensile strength and tensile modulus decreased minimally with increasing silane concentration. However, the elongation at break increased significantly (from 12.3% to 213.8%) with increasing silane concentration. The stiffness also increased with silane addition. In general, the tensile strength and tensile modulus increase with silylation of CNWs; however, the thermal properties, including the glass transition temperature, crystallinity, melting temperature, and crystallization temperature, decrease after silylation. Cellulose nanofibers (CNFs) have also been investigated in the context of PLA 3D printing. Interestingly, the method of 3D printing affects the mechanical properties of CNF-containing PLA nanocomposites [40]. Specifically, the strength and modulus of FDM-printed neat PLA is 49 and 41% lower than its compression molded counterparts. With the addition of CNFs, at just 1 wt %, the strength and modulus of 3D-printed PLA/CNFs increased by 84% and 63% compared to PLA, respectively [40]. Incorporating CNFs into PLA significantly decreased voids and facilitated nucleation and crystallization, leading to increased matrix crystallinity.

### IV. CONCLUSION

PLA is an important biodegradable polymer produced from some of the most renewable feedstocks available. While PLA is useful in FDM 3D printing, its drawbacks—brittleness, poor thermal stability, low crystallization, low elongation at break, poor impact strength, low heat distortion temperature, and limited drawability—reduce its prevalence as an industrial material. Therefore, additives have been incorporated into PLA to form nanocomposites with enhanced mechanical, electrical, or thermal properties. Cellulose is commonly incorporated into PLA matrices to enhance the mechanical properties while

maintaining complete biodegradability

## REFERENCES

1. Popescu, D. FDM process parameters influence over the mechanical properties of polymer specimens: A review. *Polym. Test.* 2018, 69, 157–166.
2. Gao, W. The status, challenges, and future of additive manufacturing in engineering. *Comput. Aided Des.* 2015, 69, 65–89.
3. Surange, V.G.; Gharat, P.V. 3D printing process using fused deposition modelling (FDM). *Int. Res. J. Eng. Technol.* 2016, 3, 1403–1406.
4. Chae, Y.; An, Y.-J. Current research trends on plastic pollution and ecological impacts on the soil ecosystem: A review. *Environ. Pollut.* 2018, 240, 387–395. [PubMed]
5. Sharma, S.; Chatterjee, S. Microplastic pollution, a threat to marine ecosystem and human health: A short review. *Environ. Sci. Pollut. Res.* 2017, 24, 21530–21547.
6. Li, W.C.; Tse, H.F.; Fok, L. Plastic waste in the marine environment: A review of sources, occurrence and effects. *Sci. Total Environ.* 2016, 566–567, 333–349. [PubMed]
7. Dinesh Kumar, S.; Venkadeshwaran, K.; Aravindan, M.K. Fused deposition modelling of PLA reinforced with cellulose nano-crystals. *Mater. Today Proc.* 2020, 33, 868–875.
8. Spinelli, G. Nanocarbon/Poly(Lactic) Acid for 3D Printing: Effect of Fillers Content on Electromagnetic and Thermal Properties. *Materials* 2019, 12, 2369.
9. Coppola, B. 3D Printing of PLA/clay Nanocomposites: Influence of Printing Temperature on Printed Samples Properties. *Materials* 2018, 11, 1947.
10. Levenhagen, N.P.; Dadmun, M.D. Interlayer diffusion of surface segregating additives to improve the isotropy of fused deposition modeling products. *Polymer* 2018, 152, 35–41.
11. Ivanov, E. PLA/Graphene/MWCNT composites with improved electrical and thermal properties suitable for FDM 3D printing applications. *Appl. Sci.* 2019, 9, 1209.
12. Caminero, M.A. Impact damage resistance of 3D printed continuous fibre reinforced thermoplastic composites using fused deposition modelling. *Compos. Part B Eng.* 2018, 148, 93–103.
13. Rajpurohit Shilpesh, R.; Dave Harshit, K. Effect of process parameters on tensile strength of FDM printed PLA part. *Rapid Prototyp. J.* 2018, 24, 1317–1324.
14. El Magri, A. Mechanical properties of CF-reinforced PLA parts manufactured by fused deposition modeling. *J. Compos. Mater.* 2019. [CrossRef]
15. Valerga, A.P. Influence of PLA Filament Conditions on Characteristics of FDM Parts. *Materials* 2018, 11, 1322.
16. Rodríguez-Panes, A.; Claver, J.; Camacho, A.M. The Influence of Manufacturing Parameters on the Mechanical Behaviour of PLA and ABS Pieces Manufactured by FDM: A Comparative Analysis. *Materials* 2018, 11, 1333.
17. Naveed, N. Investigate the effects of process parameters on material properties and microstructural changes of 3D-printed specimens using fused deposition modelling (FDM). *Mater. Technol.* 2020, 1–14. [CrossRef]
18. Huang, B. Optimizing 3D printing performance of acrylonitrile-butadiene-styrene composites with cellulose nanocrystals/silica nanohybrids. *Polym. Int.* 2019, 68, 1351–1360.

19. Farah, S.; Anderson, D.G.; Langer, R. Physical and mechanical properties of PLA, and their functions in widespread applications—A comprehensive review. *Adv. Drug Deliv. Rev.* 2016, 107, 367–392.
20. Clarkson, C.M. Crystallization kinetics and morphology of small concentrations of cellulose nanofibrils (CNFs) and cellulose nanocrystals (CNCs) melt-compounded into poly(lactic acid) (PLA) with plasticizer. *Polymer* 2020, 187, 122101.
21. Frone, A.N. Morpho-Structural, Thermal and Mechanical Properties of PLA/PHB/Cellulose Biodegradable Nanocomposites Obtained by Compression Molding, Extrusion, and 3D Printing. *Nanomaterials* 2019, 10, 51. [CrossRef] [PubMed]
22. Wilson, J.A. Magnesium catalyzed polymerization of end functionalized poly (propylene maleate) and poly (propylene fumarate) for 3D printing of bioactive scaffolds. *J. Am. Chem. Soc.* 2018, 140, 277–284. [CrossRef] [PubMed]
23. Elsayy, M.A. Hydrolytic degradation of polylactic acid (PLA) and its composites. *Renew. Sustain. Energy Rev.* 2017, 79, 1346–1352. [CrossRef]
24. Qian, S. Improved properties of PLA biocomposites toughened with bamboo cellulose nanowhiskers through silane modification. *J. Mater. Sci.* 2018, 53, 10920–10932. [CrossRef] *Nanomaterials* 2020, 10, 2567 18 of 20
25. Adesina, O.T. Mechanical property prediction of SPS processed GNP/PLA polymer nanocomposite using artificial neural network. *Cogent Eng.* 2020, 7, 1720894. [CrossRef]
26. Melocchi, A. Hot-melt extruded filaments based on pharmaceutical grade polymers for 3D printing by fused deposition modeling. *Int. J. Pharm.* 2016, 509, 255–263. [CrossRef]
27. Chacón, J.M. Additive manufacturing of PLA structures using fused deposition modelling: Effect of process parameters on mechanical properties and their optimal selection. *Mater. Des.* 2017, 124, 143–157. [CrossRef]
28. Yao, T. Tensile failure strength and separation angle of FDM 3D printing PLA material: Experimental and theoretical analyses. *Compos. Part B Eng.* 2020, 188, 107894. [CrossRef]
29. Rismalia, M. Infill pattern and density effects on the tensile properties of 3D printed PLA material. *J. Phys. Conf. Ser.* 2019, 1402, 044041. [CrossRef]
30. Vigneshwaran, K.; Venkateshwaran, N. Statistical analysis of mechanical properties of wood-PLA composites prepared via additive manufacturing. *Int. J. Polym. Anal. Charact.* 2019, 24, 584–596. [CrossRef]
31. Liao, Y. Effect of Porosity and Crystallinity on 3D Printed PLA Properties. *Polymers* 2019, 11, 1487. [CrossRef] [PubMed]
32. Wang, L.; Gardner, D.J. Contribution of printing parameters to the interfacial strength of polylactic acid (PLA) in material extrusion additive manufacturing. *Prog. Addit. Manuf.* 2018, 3, 165–171. [CrossRef]
33. Wang, L.; Gramlich, W.M.; Gardner, D.J. Improving the impact strength of Poly(lactic acid) (PLA) in fused layer modeling (FLM). *Polymer* 2017, 114, 242–248. [CrossRef]
34. Aziz, R.; Ul Haq, M.I.; Raina, A. Effect of surface texturing on friction behaviour of 3D printed polylactic acid (PLA). *Polym. Test.* 2020, 85, 106434. [CrossRef]



35. Cicala, G. Polylactide (PLA) filaments a biobased solution for additive manufacturing: Correlating rheology and thermomechanical properties with printing quality. *Materials* 2018, 11, 1191. [CrossRef]
36. Cuiffo, M.A. Impact of the Fused Deposition (FDM) Printing Process on Polylactic Acid (PLA) Chemistry and Structure. *Appl. Sci.* 2017, 7, 579. [CrossRef]
37. Patanwala, H.S. The microstructure and mechanical properties of 3D printed carbon nanotube-polylactic acid composites. *Polym. Compos.* 2018, 39, E1060–E1071. [CrossRef]
38. Long, H. Mechanical and thermal properties of bamboo fiber reinforced polypropylene/polylactic acid composites for 3D printing. *Polym. Eng. Sci.* 2019, 59, E247–E260. [CrossRef]
39. Qian, S.; Zhang, H.; Sheng, K. Cellulose nanowhiskers from moso bamboo residues: Extraction and characterization. *BioResources* 2017, 12, 419–433. [CrossRef]
40. Ambone, T.; Torris, A.; Shanmuganathan, K. Enhancing the mechanical properties of 3D printed polylactic acid using nanocellulose. *Polym. Eng. Sci.* 2020, 60, 1842–1855. [CrossRef]
41. Xiao, X. Polylactide/hemp hurd biocomposites as sustainable 3D printing feedstock. *Compos. Sci. Technol.* 2019, 184, 107887. [CrossRef]
42. Guessasma, S.; Belhabib, S.; Nouri, H. Microstructure and Mechanical Performance of 3D Printed Wood-PLA/PHA Using Fused Deposition Modelling: Effect of Printing Temperature. *Polymers* 2019, 11, 1778. [CrossRef] [PubMed]
43. Mohammadi, M. CNC dispersion in PLA and PBAT using two solvents: Morphological and rheological properties. *Cellulose* 2020, 27, 9877–9892. [CrossRef]
44. Estakhrianhaghighi, E. 3D-Printed Wood-Fiber Reinforced Architected Cellular Composites. *Adv. Eng. Mater.* 2020, 20, 2000565. [CrossRef]
45. Scaffaro, R. Lignocellulosic fillers and graphene nanoplatelets as hybrid reinforcement for polylactic acid: Effect on mechanical properties and degradability. *Compos. Sci. Technol.* 2020, 190, 108008. [CrossRef]
46. Bayraktar, I. 3D printed antibacterial silver nanowire/polylactide nanocomposites. *Compos. Part B Eng.* 2019, 172, 671–678. [CrossRef]
47. Podstawczyk, D. Preparation of antimicrobial 3D printing filament: In situ thermal formation of silver nanoparticles during the material extrusion. *Polym. Compos.* 2020, 41, 4692–4705.